

Probing inflation with CMB polarization : weak lensing effect on the covariance of CMB spectra

J Rocher^{1,2}, K Benabed² and F R Bouchet²

¹ *Theory Group, University of Texas at Austin, 1 University Station, C1608, Austin, TX 78712, USA,*

² *Institut d'Astrophysique de Paris, 98bis boulevard Arago, 75014 Paris, France.*

E-mail: rocher@physics.utexas.edu, benabed@iap.fr, bouchet@iap.fr

Abstract. CMB anisotropies are modified by the weak lensing effect of intervening large scale structures on the photon path from the last scattering surface to the observer. This has to be accounted for when observational data of sensitive experiments are used to constrain cosmological models. A common approximation to analyze the CMB angular power spectra is to include only the Gaussian part of the lensing correction and to ignore the non-gaussian terms in the error covariance matrix of the spectra. In order to investigate the validity of this approximation, we computed these non-Gaussian terms by using a perturbative expansion method. We present a graphical method to write down any N-point correlation functions at any order in lensing. We use a pedagogical approach to demonstrate that neglecting non-gaussian terms is an accurate approximation for all polarizations but B, and it will remain so even for the analysis of very sensitive post-Planck experiments. For the B polarization, non-gaussian contributions up to order 4 must be taken into account.

PACS numbers: 98.80.-k, 98.70.Vc, 98.62.Sb, 98.65.Dx

1. Introduction

Measurements of the temperature anisotropies and polarization of the Cosmic Microwave Background (CMB) provide very valuable limits and constraints on our models of the early universe [1]. This will be even more so with the increased precisions of measurements that future CMB experiments promise‡ [2]. However, while the hopes of high precision cosmology become true, second order effects that were formerly neglected or ignored have now to be taken into account. Among them, one of the most important, in particular at small angular scale, is the gravitational shear effect of the large scale structure, also commonly called the weak lensing effect [3]. This effect generates B modes [4], which are of great interest for testing theories of the early universe. Indeed, scalar primordial perturbations do not generate B modes, whose detection could therefore be considered as the “smoking gun” of the primordial gravitational wave background generically predicted by inflation theories [5]. In addition to determining the energy scale of inflation, a detection of the primordial B-mode would also test other aspects of the early universe physics, for example the presence of cosmic strings [6, 7]. From that point of view, the lensing effect is an annoying foreground limiting the detection capability of primordial B modes. It is however quite interesting in its own right, since it allows reconstructing the (projected) matter power spectrum as well as extracting information on various aspects of high energy physics such that neutrino masses [8, 9].

The gravitational deviations of photons along their paths as they cross the potential wells of the large scale structures has been studied in great details in the context of CMB. The gravitational shear shifts power between scales and creates mode couplings in the CMB power. It also deviates the distribution of temperature and polarization anisotropies from the Gaussian statistic [10]. The specific and predictable signature of the lensing effect has been used to propose various ways of detecting and reconstructing its contribution to the temperature and polarization of the CMB [11, 12, 13, 14, 15].

Until recently however, few studies had been devoted to a detailed assessment of the impact of weak lensing on the cosmological parameter estimations from CMB data. Indeed, analyzes had in general been concerned with including lensing corrections to the power spectra of CMB temperature and polarization anisotropies, but they neglected the non-gaussian corrections. Recently A. Lewis showed numerically that this approximation is valid at the sensitivity level of the Planck mission [16]. This paper presents an analysis which demonstrates that the lensing induced non-gaussian terms of the error bars on the CMB anisotropies power spectrum can be neglected as compared to the Gaussian sample variance terms except for the B-mode power spectrum. While developed independently, this works follows the line of the recently published [17, 18] and fully confirm their relevant results. Given the availability of the numerical results of these references, we rather focus here on the physical origin of the various terms by using toy models which allow understanding the final results.

Therefore, the aim of this article is in part to understand in detail the origin of

‡ <http://www.rssd.esa.int/index.php?project=Planck>

this result and above all to see whether this approximation will remain warranted in the post-Planck era, or to determine at which precision it might break down. To do so, we compute analytically the lens effect using a perturbative expansion in terms of the magnitude of the deflection field and give numerical results for the dominant order.

2. Weak lensing of the Cosmic Microwave Background anisotropies

CMB photons, as they emerge from the last scattering surface, are subject to the weak gravitational lensing effect. Measurements of the temperature anisotropies, and polarization patterns are perturbed by the cumulative effects of the large scale structure gravitational wells from $z \sim 1000$. The net result is that our measurement of temperature or polarization of the CMB in a direction \mathbf{n} in fact provides an information on photons emerging from the last scattering surface in the direction $\mathbf{n} + \xi$, ξ being the deflection induced by the gravitational shear

$$\tilde{T}(\mathbf{n}) = T(\mathbf{n} + \xi) , \quad (1)$$

$$\tilde{Q}(\mathbf{n}) = Q(\mathbf{n} + \xi) , \quad (2)$$

$$\tilde{U}(\mathbf{n}) = U(\mathbf{n} + \xi) . \quad (3)$$

In this paper, we denote by \tilde{A} the lensed appearance of any field A . The deflection ξ is the cumulative effect of all deflections produced by each gravitational well crossed during the propagation of the photon. Since those deflections are small compared to the size of the CMB anisotropies, it is sufficient to compute this cumulative effect on the unperturbed path of the photon. This approximation is often referred to as the Born approximation. By doing so, we ignore higher order corrections to the weak lensing effect, such as extra non gaussian correction of the lensing field due to the lens-lens coupling and apparition of a curl component in the spin-2 shear field. Both have been shown to be negligible in the CMB context [19].

In the Born approximation, the deflection field reduces to [10]

$$\xi(\mathbf{n}) = -2 \int_0^{\chi_{\text{cmb}}} d\chi \frac{f_K(\chi_{\text{cmb}} - \chi)}{f_K(\chi_{\text{cmb}}) f_K(\chi)} \nabla \Psi(\chi \mathbf{n}; \eta_0 - \chi) , \quad (4)$$

where $f_K(\chi)$ is the comoving angular diameter distance and Ψ the gravitational potential, linked to the density perturbation through the Poisson equation [3].

The deflection ξ being small, one can evaluate accurately the effect on the CMB field by using a perturbative expansion,

$$\tilde{X}(\mathbf{n}) = X(\mathbf{n}) + \xi_i \partial^i X(\mathbf{n}) + \frac{1}{2} \xi_i \xi_j \partial^i \partial^j X(\mathbf{n}) + \mathcal{O}(\xi^3) , \quad (5)$$

where X is either the temperature anisotropy field T or the polarization components Q or U [13, 20].

In the following, we will be interested in the effect of the gravitational shear on the properties of the power spectra of the CMB. Since our goal is only to evaluate the contribution of the non-gaussian corrections due to weak lensing, and since these corrections arise mostly at small scale, it is sufficient to work in the flat space

approximation and use a decomposition in Fourier modes rather than in spherical harmonics Y_m^l . Let us introduce the lensing potential $\phi(\mathbf{n})$ such that $\xi = \nabla\phi(\mathbf{n})$ and its Fourier transform

$$\phi(\mathbf{l}) = \int d\mathbf{n} \phi(\mathbf{n}) e^{-i\mathbf{l}\cdot\mathbf{n}}. \quad (6)$$

(5) can then be rewritten as

$$\tilde{X}_1 = \tilde{X}_1^{(0)} + \tilde{X}_1^{(1)} + \tilde{X}_1^{(2)} + \mathcal{O}(\xi^3). \quad (7)$$

When X is a scalar quantity (namely for temperature), the first and second order terms now read [20]

$$\tilde{X}_1^{(1)} = - \int \frac{d^2\mathbf{l}_1}{(2\pi)^2} X(\mathbf{l}_1) \phi(\mathbf{l} - \mathbf{l}_1) [\mathbf{l}_1 \cdot (\mathbf{l} - \mathbf{l}_1)], \quad (8)$$

$$\tilde{X}_1^{(2)} = \frac{1}{2} \int \frac{d^2\mathbf{l}_1 d^2\mathbf{l}_2}{(2\pi)^4} X(\mathbf{l}_1) \phi(\mathbf{l}_2) \phi(\mathbf{l} - \mathbf{l}_1 - \mathbf{l}_2) (\mathbf{l}_1 \cdot \mathbf{l}_2) [\mathbf{l}_1 \cdot (\mathbf{l} - \mathbf{l}_1 - \mathbf{l}_2)]. \quad (9)$$

Finally, it is convenient to use another description of the polarization field than the usual Q and U Stokes variables. Indeed, these directly observable quantities have awkward geometrical properties. They transform under rotation as the components of a spin-2 vector. One then introduces a decomposition in terms of a gradient and curl component, named E and B in analogy with the electromagnetic field decomposition, which have simpler properties under angular transformations. E is a scalar field and B a pseudo scalar one (meaning that the B polarization changes sign under a parity transformations). This decomposition has the advantage of offering an important test of the primordial cosmology model. The polarization sky pattern essentially maps the local quadrupolar temperature anisotropies on the last scattering surface and at the linear order, the scalar metric perturbations can only produce an E polarization [21]. The tensorial contribution from gravitational waves is therefore the unique source of primordial B polarization, which is concentrated at large scales. Since the tensorial contribution yields only a weak contribution to the temperature and E -type anisotropies, which is therefore very hard to detect or differentiate from the scalar part, the B modes therefore offer a potentially unique opportunity to detect a background of primordial gravitational waves, at least on the largest scales. The lensing induced B polarization may nevertheless hide the primordial contribution and is in any case dominant at small scales [10, 4].

The E and B decomposition in the flat sky approximation is easily computed from the Stokes variables through [20]

$$\pm X(\mathbf{n}) = Q(\mathbf{n}) + iU(\mathbf{n}). \quad (10)$$

Since these $\pm X$ are spin-2 quantities, their Fourier coefficients contain an additional factor $\exp[\pm 2i(\varphi_{l_1} - \varphi_l)]$. We recover the E and B Fourier coefficients with

$$\pm X(\mathbf{l}) = E(\mathbf{l}) \pm iB(\mathbf{l}), \quad (11)$$

with which we obtain that the Eqs. (8-9) translate into

$$\begin{aligned} \tilde{E}_l^{(1)} = & - \int \frac{d^2 \mathbf{l}_1}{(2\pi)^2} [E(\mathbf{l}_1) \cos(2\varphi_1) - B(\mathbf{l}_1) \sin(2\varphi_1)] \\ & \times \phi(\mathbf{l} - \mathbf{l}_1) [\mathbf{l}_1 \cdot (\mathbf{l} - \mathbf{l}_1)] , \end{aligned} \quad (12)$$

$$\begin{aligned} \tilde{B}_l^{(1)} = & - \int \frac{d^2 \mathbf{l}_1}{(2\pi)^2} [B(\mathbf{l}_1) \cos(2\varphi_1) + E(\mathbf{l}_1) \sin(2\varphi_1)] \\ & \times \phi(\mathbf{l} - \mathbf{l}_1) [\mathbf{l}_1 \cdot (\mathbf{l} - \mathbf{l}_1)] , \end{aligned} \quad (13)$$

for the first order and

$$\begin{aligned} \tilde{E}_l^{(2)} = & \frac{1}{2} \iint \frac{d^2 \mathbf{l}_1 d^2 \mathbf{l}_2}{(2\pi)^4} [E(\mathbf{l}_1) \cos(2\varphi_1) - B(\mathbf{l}_1) \sin(2\varphi_1)] \\ & \times \phi(\mathbf{l}_2) \phi(\mathbf{l} - \mathbf{l}_1 - \mathbf{l}_2) (\mathbf{l}_1 \cdot \mathbf{l}_2) [\mathbf{l}_1 \cdot (\mathbf{l} - \mathbf{l}_1 - \mathbf{l}_2)] , \end{aligned} \quad (14)$$

$$\begin{aligned} \tilde{B}_l^{(2)} = & \frac{1}{2} \iint \frac{d^2 \mathbf{l}_1 d^2 \mathbf{l}_2}{(2\pi)^4} [B(\mathbf{l}_1) \cos(2\varphi_1) + E(\mathbf{l}_1) \sin(2\varphi_1)] \\ & \times \phi(\mathbf{l}_2) \phi(\mathbf{l} - \mathbf{l}_1 - \mathbf{l}_2) (\mathbf{l}_1 \cdot \mathbf{l}_2) [\mathbf{l}_1 \cdot (\mathbf{l} - \mathbf{l}_1 - \mathbf{l}_2)] , \end{aligned} \quad (15)$$

for the second order in the perturbative development. We have used the following definition for the angles,

$$\varphi_1 \equiv \varphi_{l_1} - \varphi_l . \quad (16)$$

We can now turn to the computation of the power spectra of the CMB, C_l^{XY} , defined by

$$\langle X_l^* Y_{l'} \rangle = (2\pi)^2 \delta(\mathbf{l} - \mathbf{l}') C_l^{XY} , \quad (17)$$

where X and Y can be either T , E or B . Since no confusion can arise, from now on we shall drop the tilde on the lensed field in order to lighten notations. Putting (17) and (8-9) in (7), applying Wick theorem, and truncating the results to second order in ϕ gives [20]

$$\widetilde{C_l^{TT}} = C_l^{TT} \left(1 - \frac{l^2}{4\pi} \sigma_0^2 \right) + \frac{1}{(2\pi)^2} \int C_{l_1}^{TT} C_{|\mathbf{l}-\mathbf{l}_1|}^{\phi\phi} [\mathbf{l}_1 \cdot (\mathbf{l} - \mathbf{l}_1)]^2 d^2 \mathbf{l}_1 , \quad (18)$$

where we have defined

$$\sigma_0^2 \equiv \int_0^\infty l_1^3 C_{l_1}^{\phi\phi} dl_1 . \quad (19)$$

With the same computations, the polarization and temperature-polarization cross spectra reads

$$\begin{aligned} \widetilde{C_l^{EE}} = & C_l^{EE} \left(1 - \frac{l^2}{4\pi} \sigma_0^2 \right) + \frac{1}{(2\pi)^2} \int d^2 \mathbf{l}_1 [C_{l_1}^{EE} \cos^2(2\varphi_1) + C_{l_1}^{BB} \sin^2(2\varphi_1)] \\ & \times C_{|\mathbf{l}-\mathbf{l}_1|}^{\phi\phi} [\mathbf{l}_1 \cdot (\mathbf{l} - \mathbf{l}_1)]^2 , \end{aligned} \quad (20)$$

$$\widetilde{C_l^{BB}} = C_l^{BB} \left(1 - \frac{l^2}{4\pi} \sigma_0^2 \right) + \frac{1}{(2\pi)^2} \int d^2 \mathbf{l}_1 [C_{l_1}^{BB} \cos^2(2\varphi_1) + C_{l_1}^{EE} \sin^2(2\varphi_1)] \\ \times C_{|\mathbf{l}-\mathbf{l}_1|}^{\phi\phi} [\mathbf{l}_1 \cdot (\mathbf{l} - \mathbf{l}_1)]^2 , \quad (21)$$

and

$$\widetilde{C_l^{TE}} = C_l^{TE} \left(1 - \frac{l^2}{4\pi} \sigma_0^2 \right) + \frac{1}{(2\pi)^2} \int C_{l_1}^{TE} \cos(2\varphi_1) C_{|\mathbf{l}-\mathbf{l}_1|}^{\phi\phi} [\mathbf{l}_1 \cdot (\mathbf{l} - \mathbf{l}_1)]^2 d^2 \mathbf{l}_1 . \quad (22)$$

3. Covariance matrix of the power spectra

3.1. Gaussian assumption

Lensing is quite well known to produce non-gaussian features [22, 23, 24]. Still, in previous literature, the weak lensing effect has usually been taken into account in the partial way we recalled above. The lensing corrections have been applied to the power spectrums only; no effort have been made to reproduce the deviation from gaussianity. In other words, the effect of lensing has been reduced to a modification of the damping tails of the temperature and E power spectra, and the apparition of the small scale B induced by lensing. In that case the power spectrum covariance matrix is diagonal and reduces to the square of the C_ℓ 's of type TT , TE , EE and BB .

This approximation might turn out to be a valid one. This can be the case if the deviation from Gaussian behavior induced by lensing is small compared to the dominant Gaussian contribution, at the level of accuracy of the planned experiments. A. Cooray has argued qualitatively that this should be the case for temperature anisotropies [25]. A. Lewis has shown numerically with some mock data that this approximation holds when constraining the cosmological model at the level of precision of the upcoming Planck experiment [16]. The latter approach has the great merit that it does not make assumptions on the accuracy of the perturbative expansion used to compute the weak lensing effect on the CMB. Moreover, one can easily incorporate non-linear evolution of the matter density in the simulation and produce very accurate predictions. A downside is that such method has a relatively high computational cost and is physically less transparent.

We propose here another approach to validate the simplification described above. We evaluate analytically the impact of the non-gaussian component of the covariance matrices of the power spectrum. This provides us with a direct estimate of the extent to which the diagonal covariance matrix approximation is a valid one. To do so, we do not compute the full non-gaussian correction, and restrict ourselves to the dominant order of the lens effect within the perturbative framework introduced in the previous section.

In the simplest cases (e.g. full sky, noiseless case), one can simply estimate the cross-correlation power spectrum of two fields X and Y , by

$$\hat{C}_\ell^{XY} \equiv \frac{1}{2V_\ell} \sum_{\mathbf{l}} (X_{\mathbf{l}} Y_{\mathbf{l}}^* + X_{\mathbf{l}}^* Y_{\mathbf{l}}) = \frac{1}{V_\ell} \sum_{\mathbf{l}} X_{\mathbf{l}} Y_{\mathbf{l}}^* . \quad (23)$$

since the C_ℓ s are real. Here $X, Y = T, E, B$, $|\mathbf{l}| = \ell$ and V_ℓ is the volume of the sample of scales ℓ accessible by the experiment. These estimators of the power spectra are unbiased (in the absence of noise), and therefore $\langle \hat{C}_\ell^{XY} \rangle = C_\ell^{XY}$.

The covariance matrix of the power spectra describes how two estimators of the power spectra are correlated. It is given by

$$\text{Cov}(\ell, \ell')_{XX-YY} = \langle \hat{C}_\ell^{XX} \hat{C}_{\ell'}^{YY} \rangle - \langle \hat{C}_\ell^{XX} \rangle \langle \hat{C}_{\ell'}^{YY} \rangle. \quad (24)$$

In the case of a Gaussian random field X , and for a noise free experiment, the Wick theorem gives

$$\text{Cov}(\ell, \ell')_{XX-XX} = \frac{2}{V_\ell} [C_\ell^{XX}]^2 \delta(\ell - \ell'), \quad (25)$$

In the case where the field is sampled on the full sky, the volume V_ℓ reduces to $2\ell + 1$. Neglecting the exact shape of a survey[§], this function is often approximated by $(2\ell + 1)f_{\text{sky}}$, the f_{sky} factor being the ratio of the survey area to the full sky.

When one corrects for the experimental beam B_ℓ , and taking into account experimental noise, modeled by non-correlated white noises, one reproduce the usual formulae for the power spectrum covariances [27, 28, 29]

$$\text{Cov}(\ell)^{XX-XX} = \frac{2}{(2\ell + 1)f_{\text{sky}}} [C_\ell^{XX} + (w_x B_\ell)^{-1}]^2, \quad (26)$$

where $X = T, E, B$ and $w_{T/P}^{-1}$ denote the power spectra of non-polarized and polarized noise respectively. The diagonal term for TE is

$$\text{Cov}(\ell)^{TE-TE} = \frac{2}{(2\ell + 1)f_{\text{sky}}} \left\{ (C_\ell^{TE})^2 + [C_\ell^{TT} + (w_T B_\ell)^{-1}] [C_\ell^{EE} + (w_E B_\ell)^{-1}] \right\}. \quad (27)$$

Finally, there are three non-diagonal terms which are non zero

$$\text{Cov}(\ell)^{TT-EE} = \frac{2}{(2\ell + 1)f_{\text{sky}}} C_\ell^{TE^2}, \quad (28)$$

$$\text{Cov}(\ell)^{TT-TE} = \frac{2}{(2\ell + 1)f_{\text{sky}}} C_\ell^{TE} [C_\ell^{TT} + (w_T B_\ell)^{-1}], \quad (29)$$

and

$$\text{Cov}(\ell)^{EE-TE} = \frac{2}{(2\ell + 1)f_{\text{sky}}} C_\ell^{TE} [C_\ell^{EE} + (w_E B_\ell)^{-1}]. \quad (30)$$

[§] Of course, this is only an approximation valid in the limit of very small scales (large ℓ) as compared to the size of the survey. When this is not the case, different ℓ 's can be correlated, see the detailed work of [26].

3.2. In presence of lensing

3.2.1. Temperature If we take lensing into account, the computation above is no more valid. Indeed, we can no longer assume that the temperature and polarization obey to Gaussian distribution. The first term in the r.h.s. of (24) will translate into a four point moments that does not reduce to the usual Gaussian case through Wick expansion [22, 24].

Of course, we don't have to deal with all four point functions, but only with the reduced quantity

$$\sum_{\mathbf{l}, \mathbf{l}'} \langle X_{\mathbf{l}} Y_{\mathbf{l}}^* U_{\mathbf{l}'} V_{\mathbf{l}'}^* \rangle - \langle X_{\mathbf{l}} Y_{\mathbf{l}}^* \rangle \langle U_{\mathbf{l}'} V_{\mathbf{l}'}^* \rangle . \quad (31)$$

We use the same perturbation approach than in the previous sections, and reduce our computations to second order in lensing for all polarizations but $BB - BB$. This latter term is a particular case, for which the expansion need to be done until order four as we will develop later. We do not expect higher order terms to modify significantly our results.

To calculate at order 2 in lensing the covariance for all possible polarization, we replace each X , Y , U and V in the formula above by their second order lensed version for XY and UV taking the values TT , EE , BB , TE . Then assuming the unlensed temperature anisotropies and polarization are Gaussian, one can apply Wick theorem to compute the covariance. To simplify the computation, and since we expect the most important contribution to arise at small scale, we will keep the flat sky approximation, and assume that the volume of sample is the full plane. The complete development is given in Appendix A. We only summarize the result here.

For all $XY = UV$ covariances, we obtain two different terms. One being non-null only at $\ell = \ell'$ that we refer in the following as the diagonal or Gaussian term. The other term, being non-zero for $\ell \neq \ell'$ will be called non-diagonal or non-gaussian. In the case of the $TT - TT$ covariance, those reads respectively

$$\mathcal{D}_{\ell}^{TT-TT} = 2 (C_l^{TT})^2 \left(1 - \frac{l^2}{2\pi} \sigma_0^2 \right) + \frac{4}{(2\pi)^2} C_l^{TT} \int d^2 \mathbf{l}_1 C_{l_1}^{TT} C_{|\mathbf{l}-\mathbf{l}_1|}^{\phi\phi} [\mathbf{l}_1 \cdot (\mathbf{l} - \mathbf{l}_1)]^2 , \quad (32)$$

$$\mathcal{N}_{l,l'}^{TT-TT} = 2 \int \frac{d\varphi'}{2\pi} C_{|\mathbf{l}-\mathbf{l}'|}^{\phi\phi} \left\{ C_{l'}^{TT} [\mathbf{l}' \cdot (\mathbf{l} - \mathbf{l}')] + C_l^{TT} [\mathbf{l} \cdot (\mathbf{l}' - \mathbf{l})] \right\}^2 . \quad (33)$$

We recognize in (32) something very similar to the classical result. The diagonal part is simply the square of the lensed power spectrum, (18), truncated to second order in lensing. This is the approximation commonly used, where the power spectrum covariance with lensing are simply computed by replacing the power spectra by their lensing counterparts in (26-30). This approximation works as if the temperature anisotropies and polarization remained Gaussian, ignoring the non-diagonal contribution, (33), that describes the apparition of non-gaussian features.

3.2.2. Effects of experimental limitations We have ignored in (32-33) the experimental limitations of the considered experiment, such as the sensitivity, resolution or sky coverage. Since we are interested in the comparison between the diagonal and non-diagonal parts of the covariance matrix, these experimental limitations shouldn't affect the present work. Let us show how these quantities will enter the results given in the present work. The consequence of the introduction of the sensitivity and resolution is that the observed fluctuations are now given by

$$X_{\mathbf{l}}^{\text{obs}} = \tilde{X}_{\mathbf{l}} B_l^{1/2} + n(l) , \quad (34)$$

where $X = \{T, E, B\}$. We have assumed a Gaussian, uncorrelated noise $n(l)$ with power spectrum denoted

$$\langle n(l) n^*(l) \rangle \equiv \delta(\mathbf{l} - \mathbf{l}') w_l^{-1} \quad (35)$$

and the beam transform B_l is related to the FWHM of the beam θ_b through

$$B_l = \exp \left[-l(l+1)\theta_b^2/8 \ln 2 \right] . \quad (36)$$

As a consequence,

$$\langle X_{\mathbf{l}}^{\text{obs}} (X_{\mathbf{l}'}^{\text{obs}})^* \rangle = \delta(\mathbf{l} - \mathbf{l}') \left(\tilde{C}_l B_l + w_l^{-1}(l) \right) , \quad (37)$$

and the estimator of the *lensed* spectrum reads

$$\hat{\tilde{C}}_l \equiv B_l^{-1} \left(\int \frac{d\varphi_l}{2\pi} X_{\mathbf{l}}^{\text{obs}} (X_{\mathbf{l}}^{\text{obs}})^* - w_l^{-1} \right) . \quad (38)$$

In all the paper we will assume that the temperature noise $n_T(l)$ is uncorrelated with the signal (and with the polarized noise). Using the definition of the covariance matrix

$$\text{Cov}(l, l') \equiv \langle \hat{\tilde{C}}_l \hat{\tilde{C}}_{l'} \rangle - \langle \hat{\tilde{C}}_l \rangle \langle \hat{\tilde{C}}_{l'} \rangle \quad (39)$$

and (38), even in presence of the noise, the covariance matrix reads

$$\begin{aligned} \text{Cov}(l, l') = & \left(\int \frac{d\varphi_l}{2\pi} \frac{d\varphi_{l'}}{2\pi} \langle X_{\mathbf{l}}^{\text{obs}} (X_{\mathbf{l}}^{\text{obs}})^* X_{\mathbf{l}'}^{\text{obs}} (X_{\mathbf{l}'}^{\text{obs}})^* \rangle \right. \\ & \left. - \langle X_{\mathbf{l}}^{\text{obs}} (X_{\mathbf{l}}^{\text{obs}})^* \rangle \langle X_{\mathbf{l}'}^{\text{obs}} (X_{\mathbf{l}'}^{\text{obs}})^* \rangle \right) B_l^{-1} B_{l'}^{-1} . \end{aligned} \quad (40)$$

We can re-introduce (34), and using the fact that the noise is Gaussian and uncorrelated, we show that

$$\text{Cov}(l, l') = \int \frac{d\varphi_l}{2\pi} \frac{d\varphi_{l'}}{2\pi} \left\langle \tilde{X}_{\mathbf{l}} \tilde{X}_{\mathbf{l}}^* \tilde{X}_{\mathbf{l}'} \tilde{X}_{\mathbf{l}'}^* \right\rangle_c + 4\tilde{C}_l w_l^{-1} B_l^{-1} + 2w_l^{-2} B_l^{-2} , \quad (41)$$

where

$$\left\langle \tilde{X}_{\mathbf{l}} \tilde{X}_{\mathbf{l}}^* \tilde{X}_{\mathbf{l}'} \tilde{X}_{\mathbf{l}'}^* \right\rangle_c = \left\langle \tilde{X}_{\mathbf{l}} \tilde{X}_{\mathbf{l}}^* \tilde{X}_{\mathbf{l}'} \tilde{X}_{\mathbf{l}'}^* \right\rangle - \left\langle \tilde{X}_{\mathbf{l}} \tilde{X}_{\mathbf{l}}^* \right\rangle \left\langle \tilde{X}_{\mathbf{l}'} \tilde{X}_{\mathbf{l}'}^* \right\rangle . \quad (42)$$

Note that since the lensed anisotropies are not Gaussian, we cannot use the Wick theorem to expand the first term of (41). Rigorously, it has two contributions one

that is diagonal \mathcal{D}_ℓ and the non-diagonal term $\mathcal{N}_{l,l'}$, given by (32-33). As a conclusion, we obtain

$$\begin{aligned} \text{Cov}(l, l') &= \delta(l - l') \left[\mathcal{D}_\ell + 4\tilde{C}_l (w_l B_l)^{-1} + 2(w_l B_l)^{-2} \right] + \mathcal{N}_{l,l'} , \\ &\simeq 2\delta(l - l') \left[\tilde{C}_l + (w_l B_l)^{-1} \right]^2 + \mathcal{N}_{l,l'} . \end{aligned} \quad (43)$$

This generalizes (26). Note that the previous formulae are easily transposed to other polarization terms of the covariance by introducing a cross-correlated spectrum estimator \hat{C}_l^{TE} . We obtain generalizations of (26-30), each time introducing the quantities \mathcal{D}_ℓ and $\mathcal{N}_{l,l'}$. In the rest of the paper these quantities are calculated and compared for every polarization terms of the covariance matrix.

3.2.3. Numerical evaluation of temperature To evaluate and understand better the structure of the covariance matrix, instead of showing comparisons between numerical results for (32-33) for a few sets of cosmological parameters, we rather show results for some simple approximations of the power spectrum, with increasing complexity.

As a first step, figure 1 shows the comparison when $C_\ell = \delta(\ell - \ell_c)$, and $\ell_c = (200, 400, 800, 1600)$. This illustrates the effect of lensing on the covariance matrix for a single mode. The non-diagonal terms are at least a factor 10^{-4} below the diagonal part. We see that the lensing effect spreads the covariance matrix around the ℓ_c mode in a symmetric way; the amplitude of the effect grows with ℓ_c , the coupling between modes being more important at small scales.

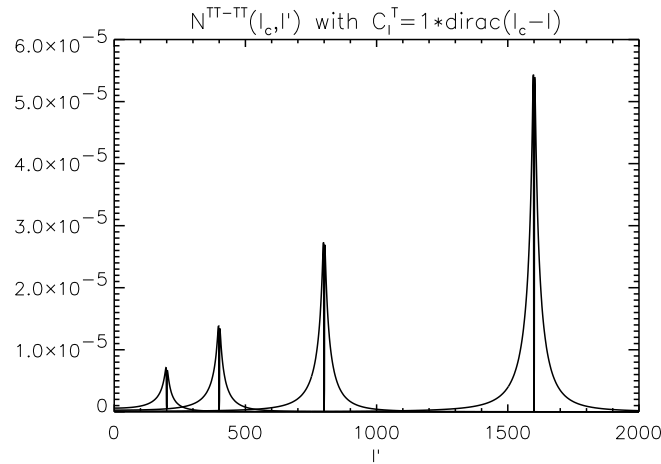


Figure 1. Non-diagonal ($l \neq l'$) contribution to the covariance matrix $\mathcal{N}_{l,l'}^{TT-TT}$ for a Dirac temperature power spectrum $C_l^{TT} = \delta(l_c - l)$ and for various values of l_c . From left to right, $l_c = 200, 400, 800$, and 1600 .

Of course, the temperature power spectra is more complicated than a Dirac function. In fact, ignoring the acoustic peaks, it is rather well described by $C_\ell^{TT} \sim \ell^{-2} \exp\left(-\frac{\ell^2}{2\ell_c^2}\right)$. We show in figure 2 the non-diagonal term for this approximation. The figure shows $l(l+1)l'(l'+1)\mathcal{N}_{ll'}$ in order to see further than the dominant variation

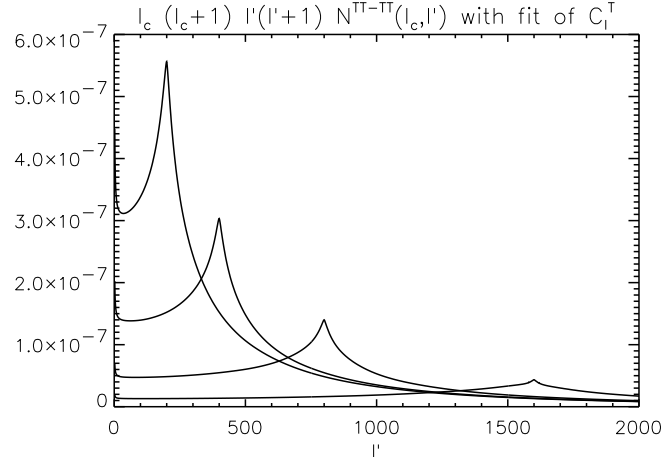


Figure 2. Non-diagonal ($l \neq l'$) contribution to the covariance matrix $\mathcal{N}_{l_c, l'}^{TT-TT}$ for a temperature power spectrum approximated by $C_l^{TT} = l^{-2} \exp\left(-\frac{l^2}{2l_c^2}\right)$ and for various values of l_c . From left to right, $l_c = 200, 400, 800$, and 1600 .

due to the ℓ^{-2} behavior of the power spectra, as is usually done with the C_ℓ . The figure exhibits the same features than the previous one. Namely it spreads over a broad range of ℓ , but with a very small amplitude. This spread is more important at large scales (small ℓ) than at small scales, which seems to contradict the idea that weak lensing is essentially a small scale effect. Of course, this is due to the exponential suppression of the small scales in the power spectrum. We showed above that the effect is essentially symmetrical.

Full results for a concordance model power spectrum are showed in figure B2, page 25, first column. It is also illustrated on figure 3 below. They display the same general features we demonstrated on our two simple examples. The structure of acoustic peaks (and especially the first one) complicates somewhat the results. However, the fact that the non-diagonal contribution is far below the diagonal part remains true.

3.2.4. Polarization terms We can perform a similar analysis for the E -type polarization. The diagonal and non-diagonal terms read (see Appendix A for a complete development)

$$\begin{aligned} \mathcal{D}_\ell^{EE-EE} = 2 (C_l^{EE})^2 \left(1 - \frac{l^2}{2\pi} \sigma_0^2 \right) + \frac{4}{(2\pi)^2} C_l^{EE} \int d^2 \mathbf{l}_1 C_{|\mathbf{l}-\mathbf{l}_1|}^{\phi\phi} & \left[C_{l_1}^{EE} \cos^2(2\varphi_1) \right. \\ & \left. + C_{l_1}^{BB} \sin^2(2\varphi_1) \right] [\mathbf{l}_1 \cdot (\mathbf{l} - \mathbf{l}_1)]^2 , \end{aligned} \quad (44)$$

$$\mathcal{N}_{l, l'}^{EE-EE} = 2 \int \frac{d\varphi'}{2\pi} C_{|\mathbf{l}-\mathbf{l}'|}^{\phi\phi} \cos^2(2\varphi') \left\{ C_{l'}^{EE} [\mathbf{l}' \cdot (\mathbf{l} - \mathbf{l}')] + C_l^{EE} [\mathbf{l} \cdot (\mathbf{l}' - \mathbf{l})] \right\}^2 . \quad (45)$$

Before giving the full numerical result for a concordance model power spectrum, we again demonstrate the features of the non-diagonal term on the simplified model $C_\ell^{EE} = \exp\left(-\frac{\ell^2}{2\ell_c^2}\right)$. figure 4 shows the corresponding result.

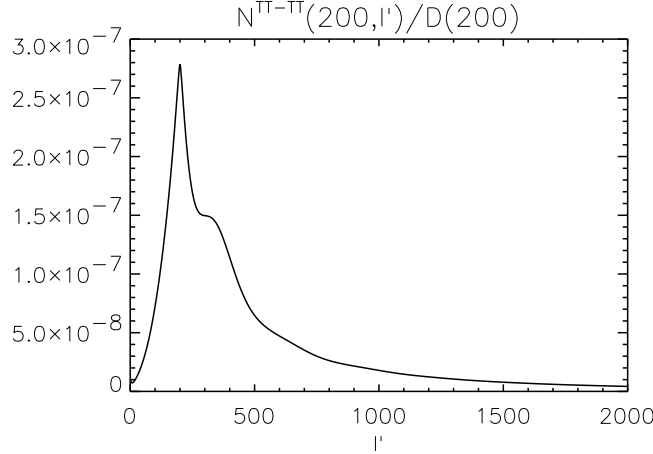


Figure 3. Non-diagonal contribution to the covariance matrix $\mathcal{N}_{200,l'}^{TT-TT}$, normalized by the diagonal value $\mathcal{D}_{200}^{TT-TT}$, and for the temperature power spectrum of the concordance model. The cosmological parameters are those measured by WMAP 3 [1].

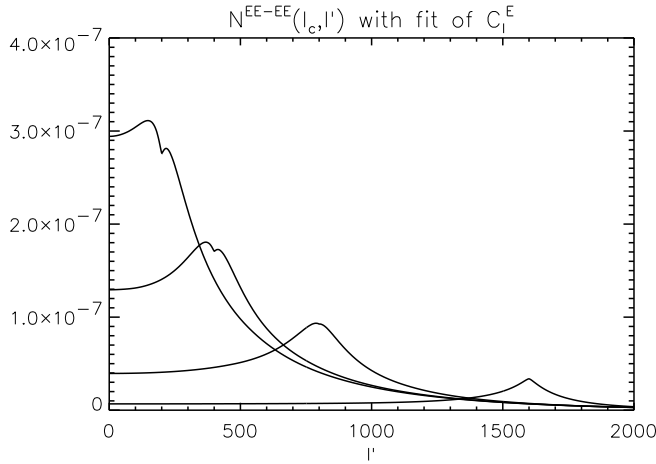


Figure 4. Non-diagonal ($l \neq l'$) contribution to the covariance matrix $\mathcal{N}_{l_c,l'}^{EE-EE}$ for a E polarization power spectrum approximated by $C_l^{EE} = \exp\left(-\frac{l^2}{2l_c^2}\right)$ and for various values of l_c . From left to right, $l_c = 200, 400, 800$, and 1600 .

The results for the full concordance model are represented in figure B2, second column. The main idea is illustrated in figure 5, where one can see the effect of the oscillations of the E spectrum and the sub-dominant amplitude of the non-diagonal contribution.

The terms for the B polarization at second order in lensing are obtained by replacing E by B and B by E in (44-45). Surprisingly, there seems to be no non-diagonal contributions from the E polarization to the covariance matrix of the B polarization. In fact, this is an artifact of the truncation of the perturbative development, which explains why $\mathcal{N}_{l,l'}^{BB-BB}$ is so small compared to the Gaussian part (see figure B2, third

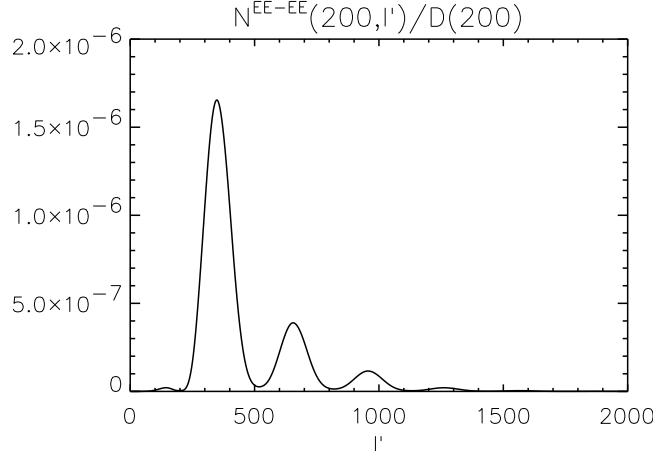


Figure 5. Non-diagonal contribution to the covariance matrix $\mathcal{N}_{200, l'}^{EE-EE}$, normalized by the diagonal value $\mathcal{D}_{200}^{EE-EE}$, and for the power spectrum of the concordance model. The cosmological parameters are those measured by WMAP 3 [1].

column). Indeed, contributions from the E mode to the B covariance cannot appear at second order (in lensing), they appear only at fourth order. Moreover, if we restrict ourselves to order 2 for the diagonal parts, there are no contribution proportional to $(C_l^{EE})^2$, which may be dominant.

It is at first sight surprising that, while doing a perturbative expansion, a 4th order term may end up being larger than a 2nd order term. The problem comes from the fact that this development is in fact done on the Q and U Stokes parameters, where second order terms are indeed greater than 4th order ones. However, we are combining these Q and U terms to form the E and B fields in a way that enhances the 4th order terms relatively to the 2nd order ones in B . The most trivial of those fourth order terms is given by the square of the second order lensed B power spectrum which contributes to the diagonal part of the covariance

$$\begin{aligned} \mathcal{D}_\ell^{BB-BB} = & (C_l^{BB})^2 \left(2 - \frac{l^2}{\pi} \sigma_0^2 \right) \\ & + \frac{4}{(2\pi)^2} C_l^{BB} \int d^2 \mathbf{l}_1 C_{|\mathbf{l}-\mathbf{l}_1|}^{\phi\phi} \left[C_{l_1}^{BB} \cos^2(2\varphi_1) + C_{l_1}^{EE} \sin^2(2\varphi_1) \right] [\mathbf{l}_1 \cdot (\mathbf{l} - \mathbf{l}_1)]^2 \\ & + \frac{2}{(2\pi)^4} \left(\int d^2 \mathbf{l}_1 C_{|\mathbf{l}-\mathbf{l}_1|}^{\phi\phi} \left[C_{l_1}^{BB} \cos^2(2\varphi_1) + C_{l_1}^{EE} \sin^2(2\varphi_1) \right] [\mathbf{l}_1 \cdot (\mathbf{l} - \mathbf{l}_1)]^2 \right)^2 \end{aligned} \quad (46)$$

This term, in addition to be the most trivial one, is also the dominant 4th order diagonal contribution. Indeed it is a configuration “1+1+1+1”, and involves therefore a term containing only E modes (contrary to configurations “2+2+0+0”, “3+1+0+0”, or “4+0+0+0”). Note that, as detailed in Appendix A, a configuration is called “1+1+1+1” when the four-point correlation function involves four fields at order 1 in lensing, see e.g. the configurations represented in figure B1.

We may think that the new diagonal term dominates the diagonal part of the covariance matrix, as lower order terms depend on the B power spectra which is much

smaller than the E modes. However, on the other hand, this term is of order four in lensing and this effect suppresses the term: it finally represents a correction of order 0.01% to the order 2.

Let us now turn to the order four non-diagonal contributions. If we assume, temporarily, that the B modes are negligible compared to E modes *at the same order in lensing*, we can see that the dominant non-diagonal 4th order terms involve four first order E modes from $\tilde{B}^{(1)}$. All possible terms of the form “1+1+1+1” are represented graphically in figure B1.

$$\mathcal{N}_{l,l'}^{BB-BB} = \frac{2}{(2\pi)^2} (A + B + C) , \quad (47)$$

where the three terms are given by

$$A = \int \frac{d\varphi'}{2\pi} \int d^2\mathbf{l}_1 \left(C_{l_1}^{EE} \right)^2 C_{|\mathbf{l}-\mathbf{l}_1|}^{\phi\phi} C_{|\mathbf{l}'-\mathbf{l}_1|}^{\phi\phi} \sin^2(2\varphi_1) \sin^2(2\varphi'_1) \times [\mathbf{l}_1 \cdot (\mathbf{l} - \mathbf{l}_1)]^2 [\mathbf{l}_1 \cdot (\mathbf{l}' - \mathbf{l}_1)]^2 , \quad (48)$$

$$B = \int \frac{d\varphi'}{2\pi} \int d^2\mathbf{l}_1 d^2\mathbf{l}_2 C_{l_1}^{EE} C_{l_2}^{EE} C_{|\mathbf{l}-\mathbf{l}_1|}^{\phi\phi} C_{|\mathbf{l}-\mathbf{l}_2|}^{\phi\phi} \sin(2\varphi_1) \sin(2\varphi'_1) \sin(2\varphi_2) \sin(2\varphi'_2) \times [\mathbf{l}_1 \cdot (\mathbf{l} - \mathbf{l}_1)] [\mathbf{l}_1 \cdot (\mathbf{l} - \mathbf{l}_2)] [\mathbf{l}_2 \cdot (\mathbf{l} - \mathbf{l}_2)] [\mathbf{l}_2 \cdot (\mathbf{l} - \mathbf{l}_1)] \delta(\mathbf{l} + \mathbf{l}' + \mathbf{l}_1 - \mathbf{l}_2) \quad (49)$$

and

$$C = \int \frac{d\varphi'}{2\pi} \int d^2\mathbf{l}_1 d^2\mathbf{l}_3 C_{l_1}^{EE} C_{l_3}^{EE} \left(C_{|\mathbf{l}-\mathbf{l}_1|}^{\phi\phi} \right)^2 \sin^2(2\varphi_1) \sin^2(2\varphi'_3) \times [\mathbf{l}_1 \cdot (\mathbf{l} - \mathbf{l}_1)]^2 [\mathbf{l}_3 \cdot (\mathbf{l} - \mathbf{l}_1)]^2 \delta(\mathbf{l} + \mathbf{l}' - \mathbf{l}_1 - \mathbf{l}_3) . \quad (50)$$

In these formulae, δ is the Dirac distribution and we have used the following definitions for the angles

$$\varphi_i \equiv \varphi_{l_i} - \varphi_l , \quad \varphi'_i \equiv \varphi_{l_i} - \varphi_{l'} . \quad (51)$$

Our results agree with those of [30, 31].

The TE-TE contributions read,

$$\begin{aligned} \mathcal{D}_\ell^{TE-TE} = & \left(C_l^{TE} \right)^2 \left(1 - \frac{l^2}{2\pi} \sigma_0^2 \right) + C_l^{TT} C_l^{EE} \left(1 - \frac{l^2}{2\pi} \sigma_0^2 \right) \\ & + \frac{1}{(2\pi)^2} C_l^{EE} \int d^2\mathbf{l}_1 C_{l_1}^{TT} C_{|\mathbf{l}-\mathbf{l}_1|}^{\phi\phi} [\mathbf{l}_1 \cdot (\mathbf{l} - \mathbf{l}_1)]^2 \\ & + \frac{1}{(2\pi)^2} C_l^{TT} \int d^2\mathbf{l}_1 [\mathbf{l}_1 \cdot (\mathbf{l} - \mathbf{l}_1)]^2 \left[C_{l_1}^{EE} \cos^2(2\varphi_1) + C_{l_1}^{BB} \sin^2(2\varphi_1) \right] C_{|\mathbf{l}-\mathbf{l}_1|}^{\phi\phi} \\ & + \frac{2}{(2\pi)^2} C_l^{TE} \int d^2\mathbf{l}_1 C_{l_1}^{TE} \cos(2\varphi_1) C_{|\mathbf{l}-\mathbf{l}_1|}^{\phi\phi} [\mathbf{l}_1 \cdot (\mathbf{l} - \mathbf{l}_1)]^2 , \end{aligned} \quad (52)$$

for the diagonal part whereas the non-diagonal part is given by

$$\begin{aligned} \mathcal{N}_{l,l'}^{TE-TE} = & \int \frac{d\varphi'}{2\pi} \left\{ \left[\left(C_{l'}^{TE} \right)^2 + C_{l'}^{EE} C_{l'}^{TT} \right] [\mathbf{l}' \cdot (\mathbf{l} - \mathbf{l}')]^2 \right. \\ & \left. + \left[\left(C_l^{TE} \right)^2 + C_l^{EE} C_l^{TT} \right] [\mathbf{l} \cdot (\mathbf{l} - \mathbf{l}')]^2 \right\} C_{|\mathbf{l}-\mathbf{l}'|}^{\phi\phi} \cos(2\varphi') \\ & + [\mathbf{l}' \cdot (\mathbf{l} - \mathbf{l}')] [\mathbf{l} \cdot (\mathbf{l} - \mathbf{l}')] \left\{ C_l^{TE} C_{l'}^{TE} [1 + \cos^2(2\varphi')] \right. \\ & \left. + \left[C_l^{EE} C_{l'}^{TT} + C_{l'}^{EE} C_l^{TT} \right] \cos(2\varphi') \right\} C_{|\mathbf{l}-\mathbf{l}'|}^{\phi\phi} . \end{aligned} \quad (53)$$

As already mentioned, until order 2 in lensing, the covariance terms involving polarization TB and EB are null. At this order, there are also no cross-correlations involving BB polarization. Thus there are no other terms in the diagonal.

We are left with six off-diagonal ($UV \neq XY$) terms. Their analytical expressions are given in Appendix B. We would like to point out that among these 6 off-diagonal terms three of them represent corrections to Gaussian terms \mathcal{D}_ℓ^{UV-XY} . But the three others involve polarization of the form $BB - XY$ with $XY \in \{TT, EE, TE\}$, polarizations for which the Gaussian terms were null. This introduces another lensing modification to the covariance matrix.

3.2.5. Numerical evaluation of the corrections Let's now turn to the numerical calculation of the non-gaussian terms ($\mathcal{N}_{l,l'}^{XY-UV}$) compared when possible to the Gaussian ones (\mathcal{D}_ℓ^{XY-UV}). This is represented in figure B2, B3, and B4. These numerical calculations mainly extend to all polarizations and to different values of multipoles the results represented for TT-TT and EE-EE in figures 3 and 5. On the figures B2 and B3, we can see that the non-gaussian contributions are completely sub-dominant compared to the Gaussian contributions, namely of the order of $10^{-2}\%$ or lower. At the end of Appendix B, in table B1, are given the absolute values of the Gaussian contribution to the covariance matrix, in order to calculate the absolute values of the non-gaussian corrections represented on figure B2, and B3. The term BBBB also receives important non-gaussian contributions from the order 4 in lensing. It has been shown in [30, 31] that these corrections are negligible at low multipoles but become important at higher multipoles ($\ell \gtrsim 800$). Despite the fact that these terms are of order four in lensing, the fact that they involve the E spectrum and not the B spectrum dominates and make these terms dominant. This is confirmed by the semi-analytical approach of A. Lewis [16]. The lensing also introduce new correlations in the covariance matrix. These terms are represented on figure B4. The amplitude of these new terms is clearly sub-dominant compared to any Gaussian term in the matrix.

Our results fully agree with those of [17, 18], although they both assumed that the primordial B modes are vanishing. However, in our calculations, we found out that this approximation is not recommended in the sense that this arbitrarily sets the second order non-diagonal contributions to the BB-BB covariance to zero. For low multipoles, these terms represent the leading corrections to the Gaussian assumption. On the other hand, one should turn to [17, 18] do see how the non-gaussian corrections propagate to the errors on cosmological parameters, and the consequences on the observation strategies.

Conclusions

CMB anisotropies and polarization data are a powerful tool to constrain the cosmological model. Indeed, their statistical properties can be computed and compared to the actual data. In the minimal case, when weak lensing is neglected, the theory predicts that, at

dominant order, the anisotropies and polarization must obey a Gaussian distribution, thus allowing the well known data compression that reduces the experimental data to a set of power spectra. This is why most article put a strong emphasis on the evaluation of the power spectra of the CMB, taking into account or not secondary effects, and reduce all experimental results to a set of C_ℓ 's. This can turn out to be a poor approximation; by doing so, one would ignore any deviation from the Gaussian behavior that can arise from those secondary effects.

We have computed analytically and numerically the Gaussian part of the covariance matrix as well as the non-gaussian contributions due to lensing. This last contribution was usually assumed to be negligible. We prove that this assumption is justified, for all polarizations except BB-BB and independently of the sensitivity of the experiment considered. The error made is always completely sub-dominant, of the order of 0.01% or lower. The covariance matrix can thus be computed using the Gaussian assumption, as described in sec. 3.1 : the covariance matrix can be computed by assuming that lensed C_l 's are Gaussian and by using the unlensed formulae (26-30), but for the replacement of the C_l 's by the lensed spectra \tilde{C}_l 's. We can see with 43 that our conclusions remain valid independently of the considered experiment, even the most sensitive one. These results confirm the recently published [17, 18] where the lensing effect on covariance has been studied as well.

The case of BB-BB polarization requires a more extended expansion in lensing, until order four, in order to take into account all dominant effects in non-gaussian corrections. Indeed, at order four, terms where only E modes contribute to the covariance matrix can exist. They have been found [30] (see also [31]) numerically dominant over Gaussian terms only when considering multipoles higher than $\ell \gtrsim 800$.

The weak lensing has another effect on the covariance matrix. It introduces new correlations between BB and TT, EE, and TE spectra. Their amplitude is strongly sub-dominant compared to any Gaussian contribution to the covariance matrix.

Acknowledgments

It is a pleasure to thank S. Prunet, J. Lesgourgues, and L. Perotto for stimulating discussions. The work of J.R. was partially supported by the National Science Foundation under Grant No. PHY-0455649, and by the University of Texas at San Antonio, Texas 78249, USA.

Appendix A. Graphical representation of different contributions to the four-point correlation function

The covariance matrix is proportional to the connected part of the four-point correlation function of the lensed anisotropy fields, defined by^{||}

$$\left\langle \tilde{X}_l \tilde{Y}_l^* \tilde{U}_{l'} \tilde{V}_{l'}^* \right\rangle_C \equiv \left\langle \tilde{X}_l \tilde{Y}_l^* \tilde{U}_{l'} \tilde{V}_{l'}^* \right\rangle - \left\langle \tilde{X}_l \tilde{Y}_l^* \right\rangle \left\langle \tilde{U}_{l'} \tilde{V}_{l'}^* \right\rangle . \quad (\text{A.1})$$

We have chosen the same Fourier transform conventions as W. Hu [20, 22], in which,

$$\langle X_{l_1} Y_{l_2}^* \rangle = (2\pi)^2 \delta(l_1 - l_2) C_{l_1}^{XY} = (2\pi)^2 \delta(l_1 - l_2) C_{l_2}^{XY} , \quad (\text{A.2})$$

for $X, Y = \phi, T, E, B$ and the four-point correlation function may be written in order to define a diagonal \mathcal{D}_l^{XY-UV} and a non-diagonal part $\mathcal{N}_{l,l'}^{XY-UV}$ as

$$\left\langle \tilde{X}_l \tilde{Y}_l^* \tilde{U}_{l'} \tilde{V}_{l'}^* \right\rangle_C = (2\pi)^4 \delta(l - l') \mathcal{D}_l^{XY-UV} + (2\pi)^2 \mathcal{N}_{l,l'}^{XY-UV} . \quad (\text{A.3})$$

For simplicity, we will illustrate our method of calculation on the $XY - UV = TT - TT$ polarization term in the covariance matrix which will clarify the various contributions to the four-point correlation function. The generalization to other polarization terms is straightforward. The method we describe here can be extended to all orders in lensing and all n -point correlation functions.

Appendix A.1. General method

Listing and calculating all contributions can be done graphically [32]: the task is then simpler and more efficient. For this, we can use the analogy with Feynman graphs. We will focus on the four-point correlation function of the temperature, up to order 2 in lensing. Let us represent by a cross \times a field $T(\ell)$ and by a circle \circ the lensing potential ϕ . The term we calculate contains two fields T at the multipole \mathbf{l} and two at the multipole \mathbf{l}' . We must remember that in general, each field \tilde{T}_l is the sum of lensed temperature field lensed at each order

$$\tilde{T}_l = T_l + \sum_{i=1}^{\infty} \tilde{T}_l^{(i)} , \quad (\text{A.4})$$

where the first $\tilde{T}^{(i)}$ are given in (8-15). This development can be represented graphically as

$$\tilde{T}_l = \times + \times \circ + \times \circ \circ + \cdots , \quad (\text{A.5})$$

As a consequence, to consider all contributions we can proceed order by order in lensing. Once the order is set (say to n), all possible combinations of the four fields \tilde{T} are written such that the sum of the four orders is equal to n . All ways of correlating them (represented by a solid line) give all the graphs contributing to the order n . Considering that we calculate the covariance matrix given in (A.1), among the fields \tilde{T} , two must be at multipole l , two at multipole l' and one field at each multipole carry a $*$ for

^{||} This definition follows the one used in previous works, for e.g. [28, 17, 30].

the complex conjugate. Then we need to use the the following rules (for temperature) derived from (8-15),

$$\begin{aligned} \times &= T, \\ \times \circ &= - \int \frac{d^2 \mathbf{l}_1}{(2\pi)^2} T(\mathbf{l}_1) \phi(\mathbf{l} - \mathbf{l}_1) [\mathbf{l}_1 \cdot (\mathbf{l} - \mathbf{l}_1)], \\ \times \circ \circ &= \frac{1}{2} \int \frac{d^2 \mathbf{l}_1 d^2 \mathbf{l}_2}{(2\pi)^4} T(\mathbf{l}_1) \phi(\mathbf{l}_2) \phi(\mathbf{l} - \mathbf{l}_1 - \mathbf{l}_2) (\mathbf{l}_1 \cdot \mathbf{l}_2) [\mathbf{l}_1 \cdot (\mathbf{l} - \mathbf{l}_1 - \mathbf{l}_2)], \end{aligned} \quad (\text{A.6})$$

where σ_0 is given by (19). Finally, we use (A.2) to calculate the contribution from the graph to the four point correlation function. Two classes of terms will appear : the diagonal ones proportional to $\delta(l - l')$ that contribute to \mathcal{D}_l^{XY-UV} and the others that contribute to $\mathcal{N}_{l,l'}^{XY-UV}$ [Note the factors (2π) due to the definition (A.3)]. To calculate the contribution to the covariance matrix, we need to introduce the integration over the angles of \mathbf{l} and \mathbf{l}' ,

$$\int \frac{d\varphi}{2\pi} \int \frac{d\varphi'}{2\pi},$$

equivalent to the summation over m and m' in the full sky calculation.

Appendix A.2. Temperature at order 0

At order 0, the graphs will not involve any \circ ; they are given in figure A1. We arbitrarily chose to put fields at multipole l in the left part of the graph and fields at multipole l' in the right part. We note that the two graphs on the first row do connect the different multipoles: they are called connected graphs. The graph on the second row is said not connected and will not contribute to the covariance matrix.

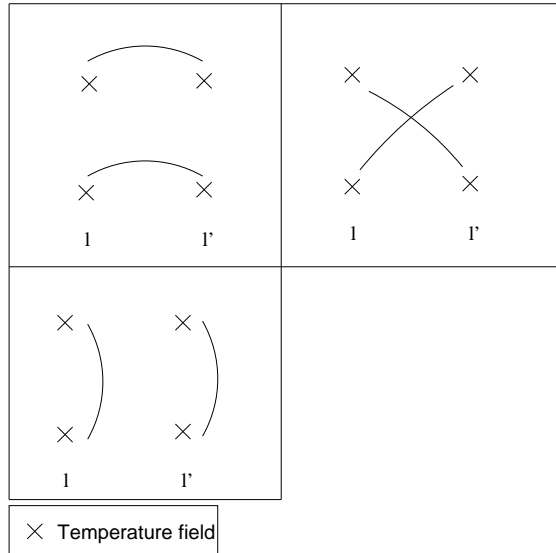


Figure A1. Configurations of correlations contributing to the order 0 of the covariance matrix.

The expression for a graph, for instance the first one of figure A1, is simply the product of the two correlations

$$\langle T_l T_{l'}^* \rangle \langle T_l^* T_{l'} \rangle = [(2\pi)^2 \delta(l - l') C_l^{TT}]^2 . \quad (\text{A.7})$$

This graph will contribute to \mathcal{D}_l . We can check that the second graph of the first row gives the same contribution and thus the total contribution to the covariance matrix of graphs of order 0 is twice the previous expression. This yields the very first term in (32).

Appendix A.3. Temperature at higher order

The contributions of order one (as well as all other odd orders) are vanishing since we are considering fields T and ϕ that are uncorrelated and of vanishing mean value

$$\langle T_l \phi_{l'} \rangle = \langle T_l \rangle = \langle \phi_l \rangle = 0 . \quad (\text{A.8})$$

Thus, in graphs with only one \circ , the lensing field cannot correlate to any other fields and one gets a term proportional to $\langle \phi \rangle$ which is null. For the same reason, all odd-point correlation functions of the CMB are null.

Let us turn to the order 2 in lensing. Graphically, we need now to add two \circ in all possible configurations (each field \tilde{T} can be expanded until order two). The easiest possibilities are to consider three unlensed temperature fields and one order 2 field. We will call this first class of graphs, the order “0+0+0+2”. Then, similarly to the figure A1, there are three ways to correlate these configurations since the two lensing fields must correlate together. For a chosen lensed field, the contributions are given in figure A2. The nine other contributions to the same order are identical but with permutations of the lensing fields.

As above, the configuration of the second row does not contribute to the covariance matrix. To calculate a term, we simply read which fields are correlated and use (A.6). For example, the first term reads

$$\begin{aligned} \langle \tilde{T}_l^{(2)} T_{l'}^* \rangle \langle T_l^* T_{l'} \rangle &= [(2\pi)^2 \delta(l - l') C_l^{TT}] \left[\frac{1}{2} \frac{1}{(2\pi)^4} \int d^2 \mathbf{l}_1 d^2 \mathbf{l}_2 \langle T_l^* T_{l_1} \rangle \langle \phi(\mathbf{l}_2) \phi(\mathbf{l}' - \mathbf{l}_1 - \mathbf{l}_2) \rangle \right. \\ &\quad \left. \times (\mathbf{l}_1 \cdot \mathbf{l}_2) [\mathbf{l}_1 \cdot (\mathbf{l}' - \mathbf{l}_1 - \mathbf{l}_2)] \right] \end{aligned} \quad (\text{A.9})$$

$$= -\frac{1}{2} (2\pi)^2 \delta(l - l') (C_l^{TT})^2 \frac{l^2}{4\pi} \sigma_0^2 , \quad (\text{A.10})$$

We can equivalently place the two lensing fields on all four temperature fields, and we can check that the second graph of first row of figure A2 give the same contribution. Thus, the total contribution to the covariance matrix of graphs of order “0+0+0+2” is 8 times the previous expression of (A.10). Finally, this term contributes to \mathcal{D}_l and gives the second (negative) term of (32).

Still restricting to the order 2 in lensing, we are now left with all the possibilities involving two temperature fields of order 1 and two unlensed fields. These graphs will

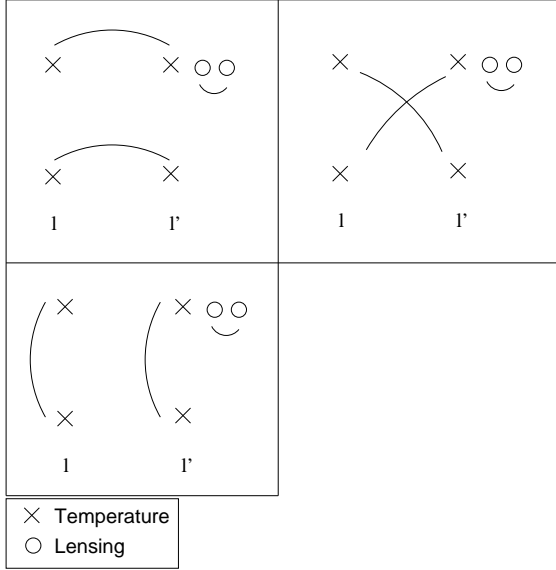


Figure A2. First set of configurations of correlations contributing to the order 2 involving three unlensed temperature fields. More precisely, they contribute to the order “0+0+0+2”.

be called the order “0+0+1+1”. To obtain all possible terms, we write graphs for all possible way of placing the lensing fields \circ : there are 6 possibilities, represented on figure A3.

Then for each graph, we write all possible ways of correlating the fields: there are still three possible ways. In total, there are 18 graphs of order “0+0+1+1”, two of them being graphs that do not contribute to the covariance matrix (unconnected graphs). Four of them are “not topologically connected” which means that they correlate the two multipoles but can be separated into two different two-point correlation functions: these graphs then contribute to \mathcal{D}_l^{TT-TT} . They give the third and last term of (32).

We are now left with 12 graphs that are either “connected” or “topologically connected”. These contributions will give new graphs that *cannot* be obtained via the product of lensed C_{ls} . Four of them are vanishing. The eight other graphs are represented in figure A4.

The two graphs of the first (resp. second) row give the contributions to $\mathcal{N}_{l,l'}^{TT-TT}$ proportional to $(C_l^{TT})^2$ (resp. $(C_{l'}^{TT})^2$) in (33). The last two rows give the contributions proportional to $C_l^{TT}C_{l'}^{TT}$.

Appendix A.4. Rules for the polarization

Let us finish this section with the few explanation for the polarization case. The method explained at the beginning of Appendix A are still valid except that the rules are slightly modified. If $+$ (resp. $-$) denotes the primordial E (resp. B) field, the rules for temperature are replaced by

$$\tilde{E}_l = +_E + +_E \circ + -_E \circ + +_E \circ \circ + -_E \circ \circ + \dots, \quad (A.11)$$

\times	$\times \circ$	$\times \circ$	\times
\times	$\times \circ$	$\times \circ$	\times
1	l'	1	l'
$\times \circ$	$\times \circ$	\times	\times
\times	\times	$\times \circ$	$\times \circ$
1	l'	1	l'
$\times \circ$	\times	\times	$\times \circ$
\times	$\times \circ$	$\times \circ$	\times
1	l'	1	l'

\times Temperature
 \circ Lensing

Figure A3. All possible configurations of temperature and lensing fields that contribute to the order “0+0+1+1”.

where for example $+_{E^\circ}$ (resp. $-_{E^\circ}$) denotes the E (resp. B) modes contributing to \tilde{E} . Once the graphs are written, their contributions can be calculated using the following rules, derived from (12-15)

$$\begin{aligned}
 +_E &= E, \\
 +_{E^\circ} &= - \int \frac{d^2 \mathbf{l}_1}{(2\pi)^2} E(\mathbf{l}_1) \cos(2\varphi_1) \phi(\mathbf{l} - \mathbf{l}_1) [\mathbf{l}_1 \cdot (\mathbf{l} - \mathbf{l}_1)], \\
 -_{E^\circ} &= \int \frac{d^2 \mathbf{l}_1}{(2\pi)^2} B(\mathbf{l}_1) \sin(2\varphi_1) \phi(\mathbf{l} - \mathbf{l}_1) [\mathbf{l}_1 \cdot (\mathbf{l} - \mathbf{l}_1)], \\
 +_{E^\circ \circ} &= \frac{1}{2} \int \frac{d^2 \mathbf{l}_1 d^2 \mathbf{l}_2}{(2\pi)^4} E(\mathbf{l}_1) \cos(2\varphi_1) \phi(\mathbf{l}_2) \phi(\mathbf{l} - \mathbf{l}_1 - \mathbf{l}_2) (\mathbf{l}_1 \cdot \mathbf{l}_2) [\mathbf{l}_1 \cdot (\mathbf{l} - \mathbf{l}_1 - \mathbf{l}_2)], \\
 -_{E^\circ \circ} &= - \frac{1}{2} \int \frac{d^2 \mathbf{l}_1 d^2 \mathbf{l}_2}{(2\pi)^4} B(\mathbf{l}_1) \sin(2\varphi_1) \phi(\mathbf{l}_2) \phi(\mathbf{l} - \mathbf{l}_1 - \mathbf{l}_2) (\mathbf{l}_1 \cdot \mathbf{l}_2) [\mathbf{l}_1 \cdot (\mathbf{l} - \mathbf{l}_1 - \mathbf{l}_2)].
 \end{aligned} \tag{A.12}$$

Using these rules, all the procedure is strictly identical to the temperature case. For example, the graphs contributing to the polarized terms of the covariance are given by the same diagrams given in figures A1, A2 and A4. The only difference is that each field contain now 2 terms from the E modes and the B modes. However a lot of terms are vanishing due to the fact that

$$\langle T_{l_1} B_{l_2}^* \rangle = \langle E_{l_1} B_{l_2}^* \rangle = 0. \tag{A.13}$$

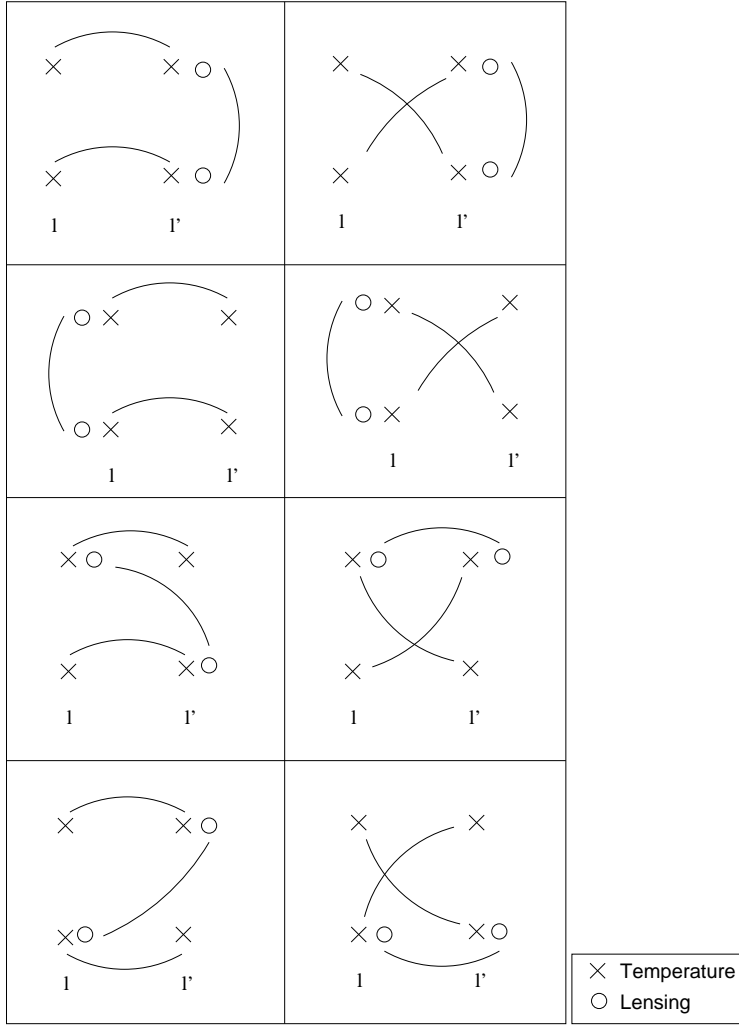


Figure A4. Non vanishing, “topologically connected”, configurations of correlations contributing to the order “0+0+1+1”. These graphs are all the contributions to $\mathcal{N}_{l,l'}^{TT-TT}$.

We can write the same expressions for the expansion of \tilde{B}_l , by replacing E by B and B by E

$$\tilde{B}_l = -_B + -_B \circ + +_B \circ + -_B \circ \circ + +_B \circ \circ + \dots, \quad (A.14)$$

At every order, clearly the main contribution will come from the the E modes denoted $+_B \circ$, $+_B \circ \circ \dots$. This diagrammatic representation is employed in section Appendix B.2 for the calculation of contributions to the covariance BB-BB at order 4 in lensing.

Appendix B. Full expressions for the covariance matrix

Appendix B.1. Cross-correlated terms of the covariance matrix at order two

We give here the expressions of the off-diagonal terms of the covariance matrix. Non-gaussian contributions $\mathcal{N}_{l,l'}^{UV-XY}$ are numerically evaluated and represented on figure B3.

They are compared to the Gaussian part \mathcal{D}_l^{UV-XY} , which is usually taken into account.

$$\begin{aligned} \mathcal{D}_l^{TT-EE} &= 2 \left(C_l^{TE} \right)^2 \left(1 - \frac{l^2}{2\pi} \sigma_0^2 \right) \\ &+ \frac{4}{(2\pi)^2} C_l^{TE} \int d^2 \mathbf{l}_1 C_{l_1}^{TE} \cos(2\varphi_1) C_{|\mathbf{l}-\mathbf{l}_1|}^{\phi\phi} [\mathbf{l}_1 \cdot (\mathbf{l} - \mathbf{l}_1)]^2 , \end{aligned} \quad (\text{B.1})$$

$$\begin{aligned} \mathcal{N}_{l,l'}^{TT-EE} &= 2 \int \frac{d\varphi'}{2\pi} \left\{ \left(C_{l'}^{TE} \right)^2 [\mathbf{l}' \cdot (\mathbf{l} - \mathbf{l}')]^2 + \left(C_l^{TE} \right)^2 [\mathbf{l} \cdot (\mathbf{l}' - \mathbf{l})]^2 \cos^2(2\varphi') \right. \\ &\left. + 2 C_l^{TE} C_{l'}^{TE} \cos(2\varphi') [\mathbf{l}' \cdot (\mathbf{l} - \mathbf{l}')] [\mathbf{l} \cdot (\mathbf{l}' - \mathbf{l})] \right\} C_{|\mathbf{l}-\mathbf{l}'|}^{\phi\phi} . \end{aligned} \quad (\text{B.2})$$

$$\begin{aligned} \mathcal{D}_l^{TT-TE} &= 2 C_l^{TT} C_l^{TE} \left(1 - \frac{l^2}{2\pi} \sigma_0^2 \right) + \frac{2}{(2\pi)^2} C_l^{TE} \int d^2 \mathbf{l}_1 C_{l_1}^{TT} C_{|\mathbf{l}-\mathbf{l}_1|}^{\phi\phi} [\mathbf{l}_1 \cdot (\mathbf{l} - \mathbf{l}_1)]^2 \\ &+ \frac{2}{(2\pi)^2} C_l^{TT} \int d^2 \mathbf{l}_1 C_{l_1}^{TE} \cos(2\varphi_1) C_{|\mathbf{l}-\mathbf{l}_1|}^{\phi\phi} [\mathbf{l}_1 \cdot (\mathbf{l} - \mathbf{l}_1)]^2 , \end{aligned} \quad (\text{B.3})$$

$$\begin{aligned} \mathcal{N}_{l,l'}^{TT-TE} &= 2 \int \frac{d\varphi'}{2\pi} \left\{ C_{l'}^{TT} C_{l'}^{TE} [\mathbf{l}' \cdot (\mathbf{l} - \mathbf{l}')]^2 + C_l^{TT} C_l^{TE} \cos(2\varphi') [\mathbf{l} \cdot (\mathbf{l}' - \mathbf{l})]^2 \right. \\ &\left. + [C_l^{TT} C_{l'}^{TE} + C_{l'}^{TT} C_l^{TE} \cos(2\varphi')] [\mathbf{l}' \cdot (\mathbf{l} - \mathbf{l}')] [\mathbf{l} \cdot (\mathbf{l}' - \mathbf{l})] \right\} C_{|\mathbf{l}-\mathbf{l}'|}^{\phi\phi} . \end{aligned} \quad (\text{B.4})$$

The last polarization terms are given by

$$\begin{aligned} \mathcal{D}_l^{EE-TE} &= 2 C_l^{TE} C_l^{EE} \left(1 - \frac{l^2}{2\pi} \sigma_0^2 \right) + \frac{2}{(2\pi)^2} C_l^{TE} \int d^2 \mathbf{l}_1 \left[C_{l_1}^{EE} \cos^2(2\varphi_1) \right. \\ &\left. + C_{l_1}^{BB} \sin^2(2\varphi_1) \right] C_{|\mathbf{l}-\mathbf{l}_1|}^{\phi\phi} [\mathbf{l}_1 \cdot (\mathbf{l} - \mathbf{l}_1)]^2 \\ &+ \frac{2}{(2\pi)^2} C_l^{EE} \int d^2 \mathbf{l}_1 C_{l_1}^{TE} \cos(2\varphi_1) C_{|\mathbf{l}-\mathbf{l}_1|}^{\phi\phi} [\mathbf{l}_1 \cdot (\mathbf{l} - \mathbf{l}_1)]^2 , \end{aligned} \quad (\text{B.5})$$

$$\begin{aligned} \mathcal{N}_{l,l'}^{EE-TE} &= 2 \int \frac{d\varphi'}{2\pi} \left\{ C_{l'}^{EE} C_{l'}^{TE} \cos^2(2\varphi') [\mathbf{l}' \cdot (\mathbf{l} - \mathbf{l}')]^2 \right. \\ &+ C_l^{EE} C_l^{TE} \cos(2\varphi') [\mathbf{l} \cdot (\mathbf{l}' - \mathbf{l})]^2 \\ &+ [C_l^{EE} C_{l'}^{TE} \cos^2(2\varphi') + C_{l'}^{EE} C_l^{TE} \cos(2\varphi')] \\ &\left. \times [\mathbf{l}' \cdot (\mathbf{l} - \mathbf{l}')] [\mathbf{l} \cdot (\mathbf{l}' - \mathbf{l})] \right\} C_{|\mathbf{l}-\mathbf{l}'|}^{\phi\phi} . \end{aligned} \quad (\text{B.6})$$

There are finally terms that are vanishing if we restrict ourselves to Gaussian terms only, involving cross terms with the B polarized spectrum. They are given by

$$\mathcal{N}_{\mathbf{l},\mathbf{l}'}^{BB-TT} = 2 \int \frac{d\varphi'}{2\pi} C_{|\mathbf{l}-\mathbf{l}'|}^{\phi\phi} \sin^2(2\varphi') C_{l'}^{TE} C_{l'}^{EE} [\mathbf{l}' \cdot (\mathbf{l} - \mathbf{l}')]^2 . \quad (\text{B.7})$$

$$\mathcal{N}_{l,l'}^{BB-EE} = 2 \int \frac{d\varphi'}{2\pi} C_{|\mathbf{l}-\mathbf{l}'|}^{\phi\phi} \left\{ C_{l'}^{BB} \sin(2\varphi') [\mathbf{l}' \cdot (\mathbf{l} - \mathbf{l}')] + C_l^{EE} \sin(2\varphi') [\mathbf{l} \cdot (\mathbf{l}' - \mathbf{l})] \right\}^2 . \quad (\text{B.8})$$

$$\begin{aligned} \mathcal{N}_{\mathbf{l}, \mathbf{l}'}^{BB-TE} = 2 \int \frac{d\varphi'}{2\pi} C_{|\mathbf{l}-\mathbf{l}'|}^{\phi\phi} \sin^2(2\varphi') \left\{ C_{l'}^{TE} C_{l'}^{EE} [\mathbf{l}' \cdot (\mathbf{l} - \mathbf{l}')]^2 \right. \\ \left. + C_{l'}^{TE} C_l^{BB} [\mathbf{l} \cdot (\mathbf{l}' - \mathbf{l})] [\mathbf{l}' \cdot (\mathbf{l} - \mathbf{l}')] \right\} . \end{aligned} \quad (\text{B.9})$$

Appendix B.2. Dominant contributions to BB-BB at order four

If we temporarily assume that the B modes are negligible compared to the E modes *at the same order in lensing*, we can see that the dominant non-diagonal 4th order terms involve four first order E modes from $\tilde{B}^{(1)}$. As explained in Appendix A, they are denoted $+_B \circ$. All possible terms of the form “1+1+1+1” are represented graphically in figure B1. For each column, the two graphs have the same contribution, respectively

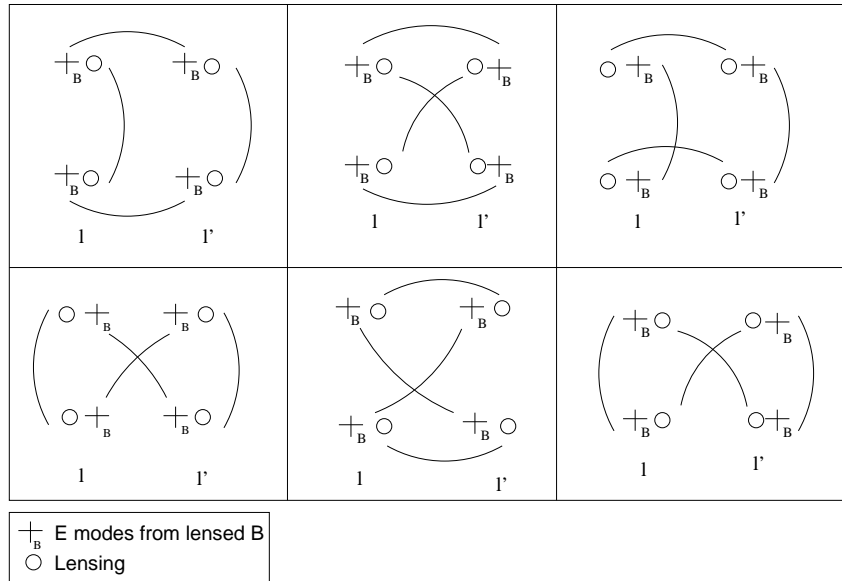


Figure B1. Non-diagonal “topologically connected” configurations of correlations contributing to the covariance matrix, for the polarization BB-BB at order “1+1+1+1”. These graphs are the dominant terms contributing to $\mathcal{N}_{\mathbf{l}, \mathbf{l}'}^{BB-BB} (4)$ at order four in lensing.

given by (48-50).

Appendix B.3. Numerical calculation of the non-gaussian contributions

We now turn to the numerical calculation of all these terms. They are represented on the following figures B2, B3, and B4. When possible (figures B2, and B3) these non-gaussian corrections are renormalized by the Gaussian value \mathcal{D}_ℓ^{XY-UV} so that the amplitude of the graph reflects the amplitude of the correction. These renormalization factors are given in Table B1. This table can be used to evaluate the absolute amplitude of non-gaussian corrections of figures B2, and B3 and can then be compared to the corrections of figure B4.

Multipole	$TT - TT$	$EE - EE$	$BB - BB$	$TE - TE$	$TT - TE$	$TT - EE$	$EE - TE$
$\ell = 200$	2.6×10^7	11	7.2	8.4×10^3	5.2×10^4	10^2	34
$\ell = 400$	2.4×10^6	9.2×10^2	1.4×10^2	2.3×10^4	2.0×10^4	1.6×10^2	3.9×10^2
$\ell = 800$	5.5×10^6	6.7×10^3	4.9×10^3	9.8×10^4	1.3×10^5	2.8×10^3	4.4×10^3
$\ell = 1600$	4.3×10^5	1.2×10^6	1.2×10^6	3.7×10^5	1.1×10^4	2.8×10^2	1.9×10^4

Table B1. Absolute values of the covariance matrix in the Gaussian limit \mathcal{D}_ℓ^{XY-UV} with the pre-factor $[\ell(\ell+1)/2\pi]^2$. The unit is $(\mu K)^4$.

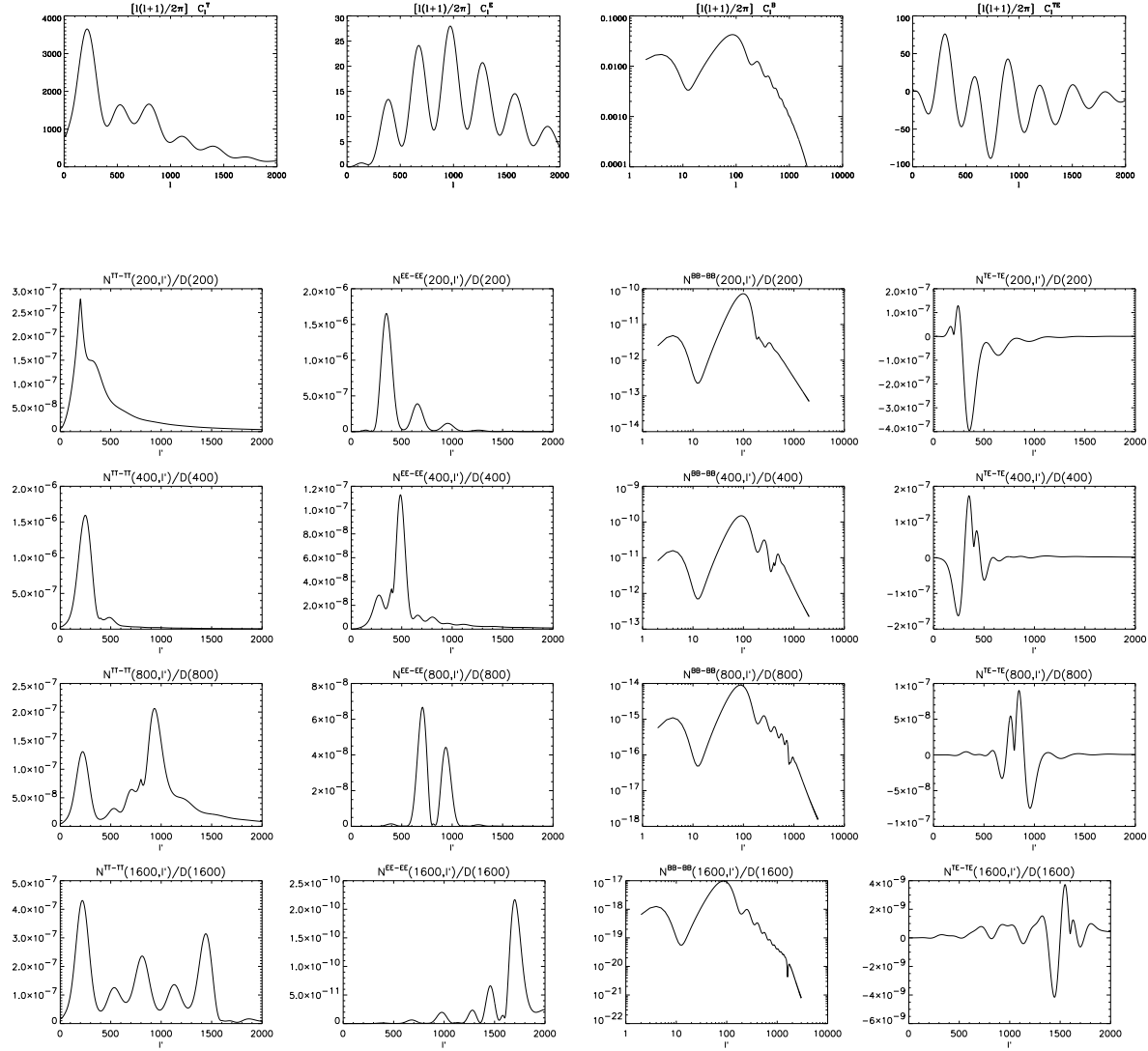


Figure B2. On the first row, we recall the form of the TT, EE, BB, and TE power spectrum in the absence of lensing. The cosmological parameters are given by WMAP 3 [1] and we assume a tensor/scalar ratio $r = 1$. Below is the non-diagonal ($l \neq l'$) contribution to the covariance matrix $\mathcal{N}_{l,l'}^{UV-XY}$ for several polarization and various values of l . From left to right, $UV - XY = TT - TT$, $EE - EE$, $BB - BB$, and $TE - TE$, and from top to bottom, $l = 200, 400, 800$, and 1600 . The amplitude is normalized to by the diagonal value D_l^{UV-XY} to have the relative contribution.

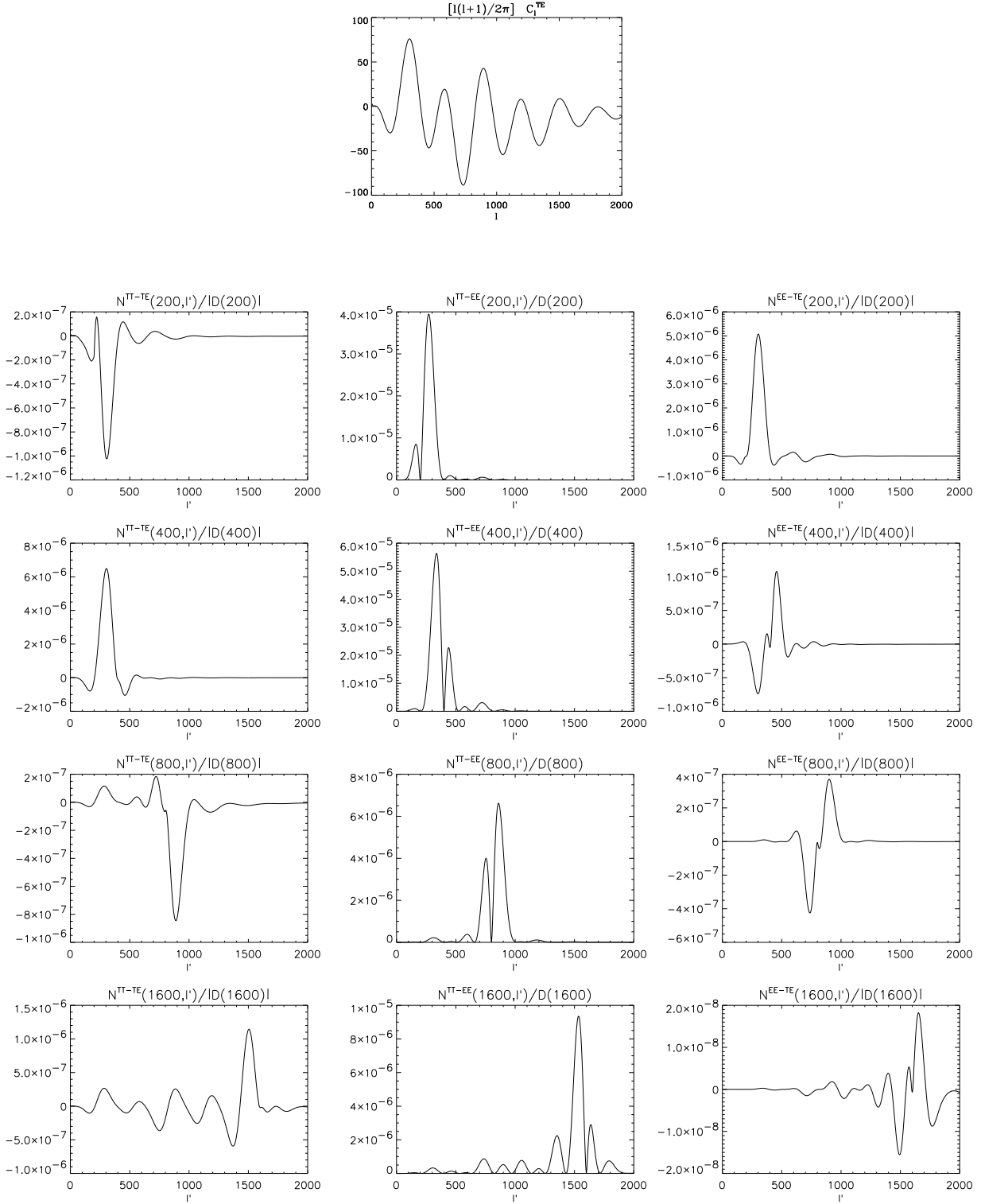


Figure B3. Non-diagonal ($l \neq l'$) contribution to the covariance matrix $\mathcal{N}_{l,l'}^{UV-XY}$ for several polarization and various values of l . From left to right, $UV - XY = TT - EE$, $TT - TE$, and $EE - TE$, and from top to bottom, $l = 200, 400, 800$, and 1600 . The amplitude is normalized to the diagonal value \mathcal{D}_l^{UV-XY} to have the relative contribution. Above the middle column we represent the cross correlated spectrum C_l^{TE} , since it is the only spectrum that generates the term $\mathcal{N}_{l,l'}^{TT-EE}$. The cosmological parameters are given by WMAP 3 [1] and we assume a tensor/scalar ratio $r = 1$.

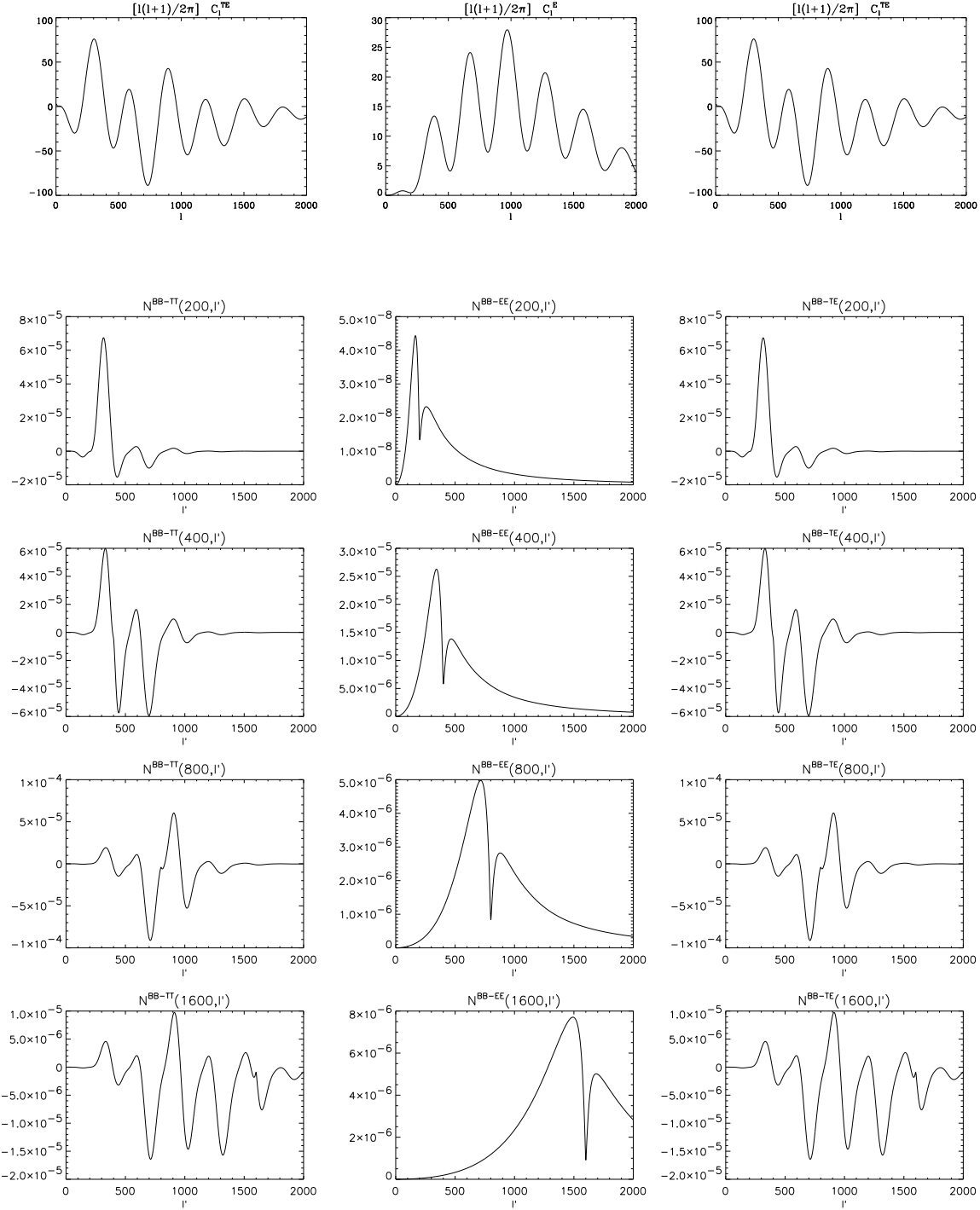


Figure B4. Non-diagonal ($l \neq l'$) contribution to the covariance matrix $\mathcal{N}_{l,l'}^{UV-XY}$ for several polarization and various values of l . From left to right, $UV - XY = BB - TT$, $BB - EE$, and $BB - TE$, and from top to bottom, $l = 200, 400, 800$, and 1600 . The amplitude is not renormalized by any Gaussian value since these terms are vanishing in the Gaussian limit. On the first line are represented the C_l s that play the most important role in the non-diagonal contribution below. The cosmological parameters are given by WMAP 3 [1] and we assume a tensor/scalar ratio $r = 1$.

References

- [1] Spergel D N *et al.* Wilkinson Microwave Anisotropy Probe (WMAP) Three Year Results: Implications for Cosmology. *ArXiv Astrophysics e-prints*, March 2006.
- [2] Bock J *et al.* Task Force on Cosmic Microwave Background Research. *ArXiv Astrophysics e-prints*, April 2006.
- [3] Bartelmann M and Schneider P. Weak gravitational lensing. *Phys. Rept.*, 340:291–472, 2001.
- [4] Zaldarriaga M and Seljak U. Gravitational lensing effect on cosmic microwave background polarization. *Phys. Rev. D*, 58(2):023003–+, July 1998.
- [5] Kinney W H. Constraining inflation with cosmic microwave background polarization. *Phys. Rev.*, D58:123506, 1998.
- [6] Seljak U and Slosar A. B polarization of cosmic microwave background as a tracer of strings. *Phys. Rev.*, D74:063523, 2006.
- [7] Wasserman I Pogosian L and Wyman M. On vector mode contribution to CMB temperature and polarization from local strings. *ArXiv Astrophysics e-prints*, April 2006.
- [8] Pastor S Lesgourgues J, Perotto L and Piat M. Probing neutrino masses with cmb lensing extraction. *Phys. Rev.*, D73:045021, 2006.
- [9] Lesgourgues J and Pastor S. Massive neutrinos and cosmology. *Phys. Rept.*, 429:307–379, 2006.
- [10] Lewis A and Challinor A. Weak gravitational lensing of the cmb. *Phys. Rept.*, 429:1–65, 2006.
- [11] Hirata C M and Seljak U. Reconstruction of lensing from the cosmic microwave background polarization. *Phys. Rev. D*, 68(8):083002–+, October 2003.
- [12] Okamoto T and Hu W. Cosmic microwave background lensing reconstruction on the full sky. *Phys. Rev. D*, 67(8):083002–+, April 2003.
- [13] Bernardeau F Benabed K and van Waerbeke L. CMB B polarization to map the large-scale structures of the universe. *Phys. Rev. D*, 63(4):043501–+, February 2001.
- [14] Bernardeau F Van Waerbeke L and Benabed K. Lensing Effect on the Relative Orientation between the Cosmic Microwave Background Ellipticities and the Distant Galaxies. *Astrophysical Journal*, 540:14–19, September 2000.
- [15] Zaldarriaga M and Seljak U. Reconstructing projected matter density power spectrum from cosmic microwave background. *Phys. Rev. D*, 59(12):123507–+, June 1999.
- [16] Lewis A. Lensed cmb simulation and parameter estimation. *Phys. Rev.*, D71:083008, 2005.
- [17] Smith K M, Hu W, and Kaplinghat M. Cosmological information from lensed CMB power spectra. *Phys. Rev. D*, 74(12):123002–+, December 2006.
- [18] Li C, Smith T L, and Cooray A. Non-Gaussian Covariance of CMB B-modes of Polarization and Parameter Degradation. *Phys. Rev. D*, 75:083501, 2007.
- [19] Shapiro C and Cooray A. The Born and lens lens corrections to weak gravitational lensing angular power spectra. *Journal of Cosmology and Astro-Particle Physics*, 3:7–+, March 2006.
- [20] Hu W. Weak Lensing of the CMB: A Harmonic Approach. *Phys. Rev. D*, 62(4):043007–+, July 2000.
- [21] Hu W and Dodelson S. Cosmic Microwave Background Anisotropies. *Annu. Rev. Astron. and Astrophys.*, 40:171–216, 2002.
- [22] Hu W. Angular trispectrum of the cosmic microwave background. *Phys. Rev. D*, 64(8):083005–+, October 2001.
- [23] Zaldarriaga M. Lensing of the CMB: Non-Gaussian aspects. *Phys. Rev. D*, 62(6):063510–+, September 2000.
- [24] Bernardeau F. Weak lensing detection in CMB maps. *Astronomy and Astrophysics*, 324:15–26, August 1997.
- [25] Cooray A. Weak lensing of the cosmic microwave background: Power spectrum covariance. *Phys. Rev. D*, 65(6):063512–+, March 2002.
- [26] Challinor A and Chon G. Error analysis of quadratic power spectrum estimates for cmb polarization: sampling covariance. *Mon. Not. Roy. Astron. Soc.*, 360:509–532, 2005.

- [27] Seljak U. Measuring polarization in cosmic microwave background. *ArXiv Astrophysics e-prints*, 1996.
- [28] Zaldarriaga M and Seljak U. An all-sky analysis of polarization in the microwave background. *Phys. Rev.*, D55:1830–1840, 1997.
- [29] Kosowsky A Kamionkowski M and Stebbins A. A probe of primordial gravity waves and vorticity. *Phys. Rev. Lett.*, 78:2058–2061, 1997.
- [30] Hu W Smith K M and Kaplinghat M. Weak lensing of the CMB: Sampling errors on B modes. *Phys. Rev. D*, 70(4):043002–+, August 2004.
- [31] Challinor A Smith S and Rocha G. What can be learned from the lensed cosmic microwave background b-mode polarization power spectrum? *Phys. Rev.*, D73:023517, 2006.
- [32] Gaztanaga E Bernardeau F, Colombi S and Scoccimarro R. Large-scale structure of the universe and cosmological perturbation theory. *Phys. Rept.*, 367:1–248, 2002.